On the triggering of Benguela Niños: Remote equatorial versus local influences

Ingo Richter,[1] Swadhin K. Behera,[1] Yukio Masumoto,[1] Bunmei Taguchi,[2]
Nobumasa Komori,[2] and Toshio Yamagata[3,4]

Received 23 June 2010; revised 2 September 2010; accepted 16 September 2010; published 26 October 2010.

[1] The relative importance of remote and local influences in the development of Benguela Niños is examined using observations and a coupled general circulation model capable of simulating interannual variability in the tropical Atlantic. While previous studies have emphasized the role of equatorially excited Kelvin waves, the present study finds that meridional wind anomalies along the southwest African coast contribute substantially. Both observations and model output indicate that sea-surface temperatures along the southwest African coast respond rapidly to changes in meridional wind stress. These wind anomalies form part of a basin-scale weakening of the subtropical anticyclone that extends to the equator. As the weakening begins three months before the peak of the event it might have some predictive potential. Results also indicate that the close correlation between Benguela and Atlantic Niños in observations might result from the large spatially coherent wind stress anomalies associated with the weakened anticyclone. **Citation:** Richter, I., S. K. Behera, Y. Masumoto, B. Taguchi, N. Komori, and T. Yamagata (2010), On the triggering of Benguela Niños: Remote equatorial versus local influences, *Geophys. Res. Lett.*, *37*, L20604, doi:10.1029/2010GL044461.

1. Introduction

[2] Sea surface temperatures (SSTs) along the coast of southwestern Africa undergo fluctuations on interannual to decadal time scales. Because of their similarity with SST fluctuations along the South American coast associated with El Niño/Southern Oscillation and due to their location in the Angola/Benguela upwelling region, warm events have been termed Benguela Niños [*Shannon et al.*, 1986]. They are marked by a reduction in upwelling and the poleward intrusion of warm equatorial waters, which leads to a decrease in biological productivity and can have severe consequences for local fisheries but also influences precipitation over southwest Africa [*Shannon et al.*, 1986; *Reason and Rouault*, 2006]. Skillful prediction of these events is thus of great importance.

[3] The study of *Shannon et al.* [1986] found that changes in local along-shore winds cannot explain SST variations in the Angola/Benguela area (ABA; here defined as the region 25°S–15°S, 8°E-coast). Instead they suggested that wind stress anomalies to the north, and possibly in the equatorial Atlantic, are the dominant factor. While two recent studies by *Polo et al.* [2008a, 2008b] point out that the influence of Kelvin waves might not reach further poleward than 12°S and thus not affect the ABA, most other studies have made the case for remote equatorial influences on the ABA [*Florenchie et al.*, 2003, 2004; *Grodsky et al.*, 2006; *Huang and Hu*, 2007; *Rouault et al.*, 2007]. More specifically, these latter studies hypothesize that zonal wind stress anomalies in the equatorial Atlantic trigger Kelvin waves that propagate along the equator and subsequently along the southwest African coast where they induce downwelling anomalies. Such a mechanism was first proposed to explain the annual cycle in the Gulf of Guinea [*Moore et al.*, 1978] and the Angola Dome [*Yamagata and Iizuka*, 1995]. The remote forcing mechanism could allow prediction of Benguela Niños by monitoring equatorial conditions but, due to the small basin size, lead times might be rather short, depending on which modes are involved. Observed phase speeds typically range between 1.5–2 m/s [e.g., *Polo et al.*, 2008a], suggestive of the second baroclinic mode. This would mean that a Kelvin wave excited in the central equatorial Atlantic would reach the ABA in about 30–40 days.

[4] Where and how Benguela Niños are forced, has important implications for their prediction. If the forcing region lies in the equatorial Atlantic, then observations like those from the Prediction and Research Moored Array in the Tropical Atlantic (PIRATA) [*Servain et al.*, 1998; *Bourlès et al.*, 2008] can supply valuable information. If, on the other hand, these events arise from local wind stress anomalies, monitoring and prediction efforts should focus on oceanic and atmospheric conditions along the southwest African coast.

[5] The present study aims to clarify the factors contributing to the evolution of Benguela Niños. Using a coupled general circulation model (GCM) described in section 2, we will show in section 3 that, in the context of the model simulation, wind stress anomalies along the southwest African coast play a crucial role in the development of these events. We will further show that the along-shore wind anomalies form part of a basin-scale weakening of the subtropical anticyclone. These model results are also backed up by the observations presented in section 3. The implications of our results are given in section 4.

2. Model Experiment and Observational Data Sets

[6] In this study we partly rely on output from a coupled GCM (CGCM), which has the advantage of providing a

[1]Research Institute for Global Change and Application Laboratory, JAMSTEC, Yokohama, Japan.
[2]Earth Simulator Center, JAMSTEC, Yokohama, Japan.
[3]Department of Earth and Planetary Sciences, University of Tokyo, Tokyo, Japan.
[4]Application Laboratory, JAMSTEC, Yokohama, Japan.

0094-8276/10/2010GL044461

long-term record of SST and surface winds, for which the satellite observation period is short. The model used in this study is the CGCM for the Earth Simulator (CFES), which consists of the atmospheric GCM for the Earth Simulator (AFES3) [*Kuwano-Yoshida et al.*, 2010; *Enomoto et al.*, 2008; *Ohfuchi et al.*, 2004] and the Coupled Ocean-Sea Ice Model for the Earth Simulator (OIFES) [*Komori et al.*, 2005]. AFES3 is based on the Center for Climate System Research (CCSR)/National Institute for Environmental Studies (NIES) AGCM 5.4.02 [*Numaguti et al.*, 1997], while OIFES is based on the Modular Ocean Model version 3 (MOM3) [*Gnanadesikan et al.*, 2006]. Further details of CFES are given by *Nonaka et al.* [2009] and *Komori et al.* [2008]. The CFES integration analyzed in this study was run at a resolution of T119 (~1°) and 48 σ-levels in the atmosphere, and 0.5° and 54 vertical levels in the ocean. The model was integrated for 120 years of which the last 96 are analyzed here.

[7] CFES achieves a rather realistic simulation of the tropical Atlantic where many state-of-the-art CGCMs still suffer serious biases [*Davey et al.*, 2002; *Richter and Xie*, 2008]. In the climatological mean, CFES SST biases along the equatorial Atlantic are typically less than 1.5 K (not shown). While CFES' SSTs in the ABA are up to 3.5 K warmer than observed, it compares more favorably with observations than AR4 models and also manages to capture the seasonal cycle (see Figure S1a in Text S1 of the auxiliary material).[1] Mean depth and seasonal cycle of the 15°C isotherm are also well captured (Figure S1b in Text S1 of the auxiliary material). In terms of tropical Atlantic variability, CFES simulates Atlantic and Benguela Niños (as well as their Niña counterparts) with realistic amplitude and frequency. The model also reproduces, with the exception of a spurious peak in June, the observed seasonal phase locking, namely a major peak in boreal spring and a minor peak in boreal fall (Figure S2 in Text S1 of the auxiliary material). CFES' relatively successful simulation of tropical Atlantic variability makes it a useful tool to study the evolution of Benguela Niños and Niñas though here the focus will be on the former.

[8] On the observational side, we use satellite observations of AVHRR SST and QuikSCAT surface winds at 0.25° resolution, and AVISO sea surface height (SSH) at 1/3° resolution for the period 1993–2008. We supplement these observational data with reanalysis data from the European Center for Medium Range Weather Forecasting (ECMWF) ERA40 (period 1958–2001 inclusive; regridded to 2.5°) and the Simple Ocean Assimilation (SODA; *Carton et al.* [2000]; period 1958–2007 inclusive; regridded to 2°).

3. Results

[9] To track the evolution of Benguela Niños we plot composited monthly anomalies as longitude-time sections along the equator, averaged between 2°S–2°N (Figure 1a), and latitude-time sections along the southwest African coast (Figure 1b), where only ocean points between the coast and 4° offshore are selected. The spatial and temporal resolutions are chosen to show the general sequence of events rather than to track the propagation of Kelvin waves, which will be examined later in this section. Compositing is performed by selecting the 13 events for which AB1 SST anomalies exceed 2 standard deviations. Latitude-time sections of anomalous upper ocean heat content (integrated from 0 to150 m depth) and meridional wind stress (Figure 1b) indicate that there is a high degree of correspondence between these two fields along the southwestern African coast. Positive heat content anomalies appear 7 months before the peak of the composite event and are accompanied by northerly (downwelling favorable) wind stress anomalies. In the central and eastern equatorial Atlantic, on the other hand, positive heat content anomalies develop 1–2 months later and thus appear to be dynamically unrelated to the onset of the Benguela Niño. Subsequently, the equatorial warm anomalies appear to propagate eastward and southward toward the ABA and likely strengthen the event. Note, however, that the most pronounced heat and westerly wind anomalies on the equator develop one month after the peak of the event.

[10] The same analysis performed on 50 years of SODA reanalysis yields rather similar results (Figure S3 in Text S1 of the auxiliary material) though, in the developing stage, the equatorial influence appears more prominent. A westerly wind anomaly develops over the eastern equatorial Atlantic about 8 months before the peak of the event and is accompanied by a southward propagating heat content anomaly. While the propagation speed of approximately 0.3 m/s appears too slow for the first few Kelvin modes it is evident that these heat content anomalies contribute to the subsequent development of the event in the SODA composites. Despite these differences with CFES results in the pre-onset phase, the rapid development that starts 3 months prior to the peak is very similar to the CFES composite (Figures 1a and 1b) and displays the same close correspondence between northerly wind and heat content anomalies.

[11] To examine the basin-wide changes associated with warm events we plot horizontal maps of SST, surface wind stress, and sea level pressure (SLP) anomalies (Figure 2a), composited in the same way as above. Three months before the peak of the composite event, both the equatorial easterlies and the along-shore southerly winds are noticeably weakened and this is accompanied by a decrease in SLP south of 20°S. SST anomalies are confined to the Namibian coast at 20°S and do not exceed 1 K. Two months later, wind stress anomalies cover the whole South Atlantic basin and show a weakening of the southeast trade winds, the equatorial easterlies, and the along-shore winds. The concomitant SLP anomalies suggest a basin-scale weakening of the subtropical anticyclone, with the surface wind anomalies roughly aligned with the isobars. SST anomalies around 20°S have spread further westward and reach almost 2 K at the coast. During the peak month, when the SST anomaly in the ABA matures, the equatorial cold tongue region also experiences significant warming, suggestive of an incipient Atlantic Niño. This is consistent with the tendency of Atlantic Niños to follow Benguela Niños.

[12] The ERA 40 reanalysis reveals a similar evolution of SST and surface wind anomalies (Figure S4 in Text S1 of the auxiliary material) although the weakening of the subtropical anticyclone is less organized than in the simulation, possibly due to the shorter analysis period (1958–2001) and inconsistencies among assimilated fields.

[1] Auxiliary materials are available in the HTML. doi:10.1029/2010GL044461.

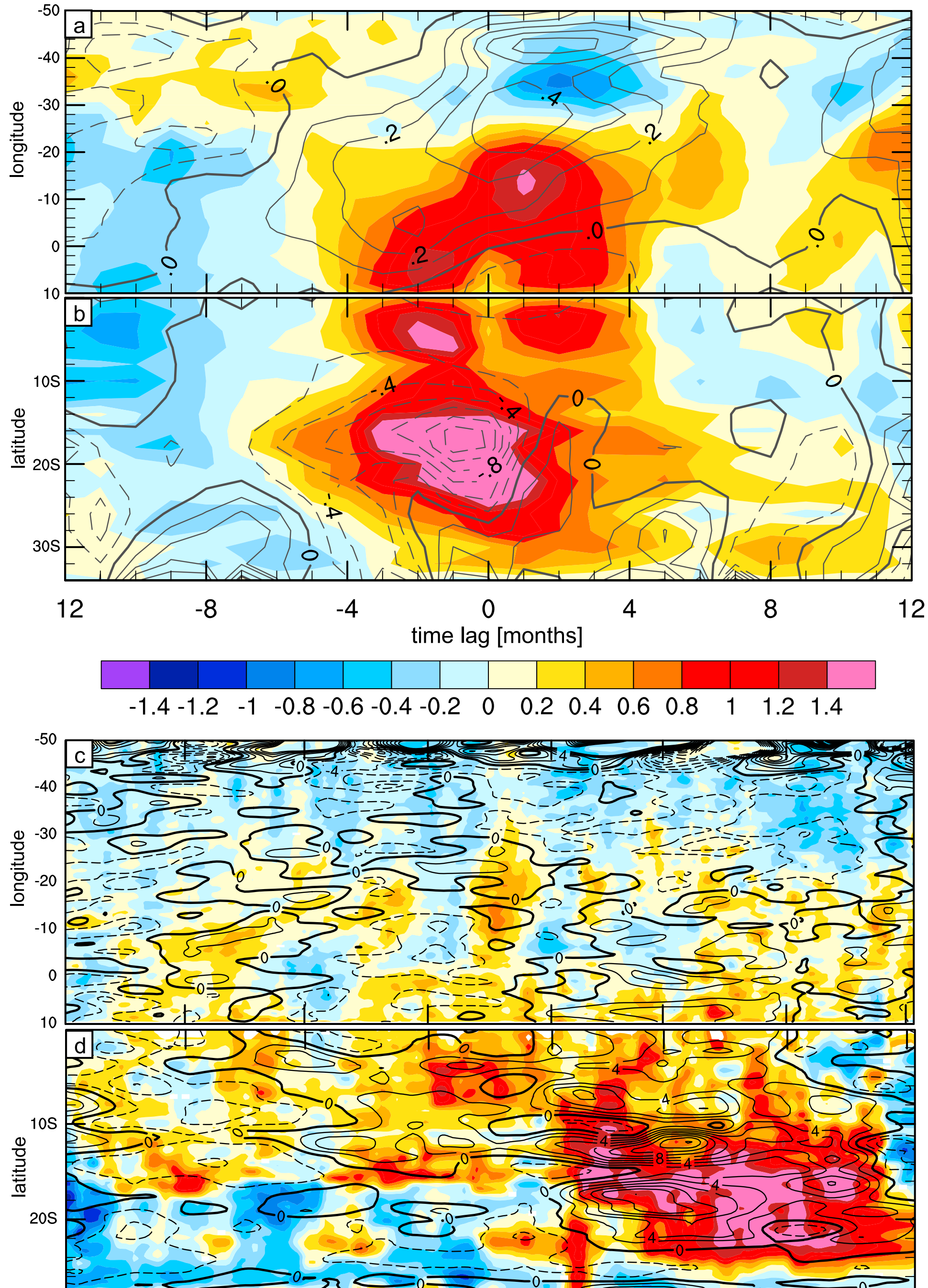

Figure 1. Time sections of (a) CFES composites of upper ocean heat content (shading; J/m*E14) and zonal wind stress (contours; N m^{-2}*100; interval 0.1) along the equator, (b) CFES composites of upper ocean heat content (shading; J/m*E14) and meridional wind stress (contours; N m^{-2}*100; interval 0.2) along the southwest African coast, (c) AVHRR SST (shading; K) and AVISO sea surface height (contours; cm; interval 2) along the equator, and (d) AVHRR SST (shading; K) and AVISO sea surface height (con-tours; cm; interval 2) along the southwest African coast. The composites in Figures 1a and 1b are based on events for which the ABA SST anomaly exceeds +2 standard deviations. The abscissa for Figures 1a and 1b indicates the month relative to the peak of the composite event. The AVHRR and AVISO satellite observations are for year 1994/1995.

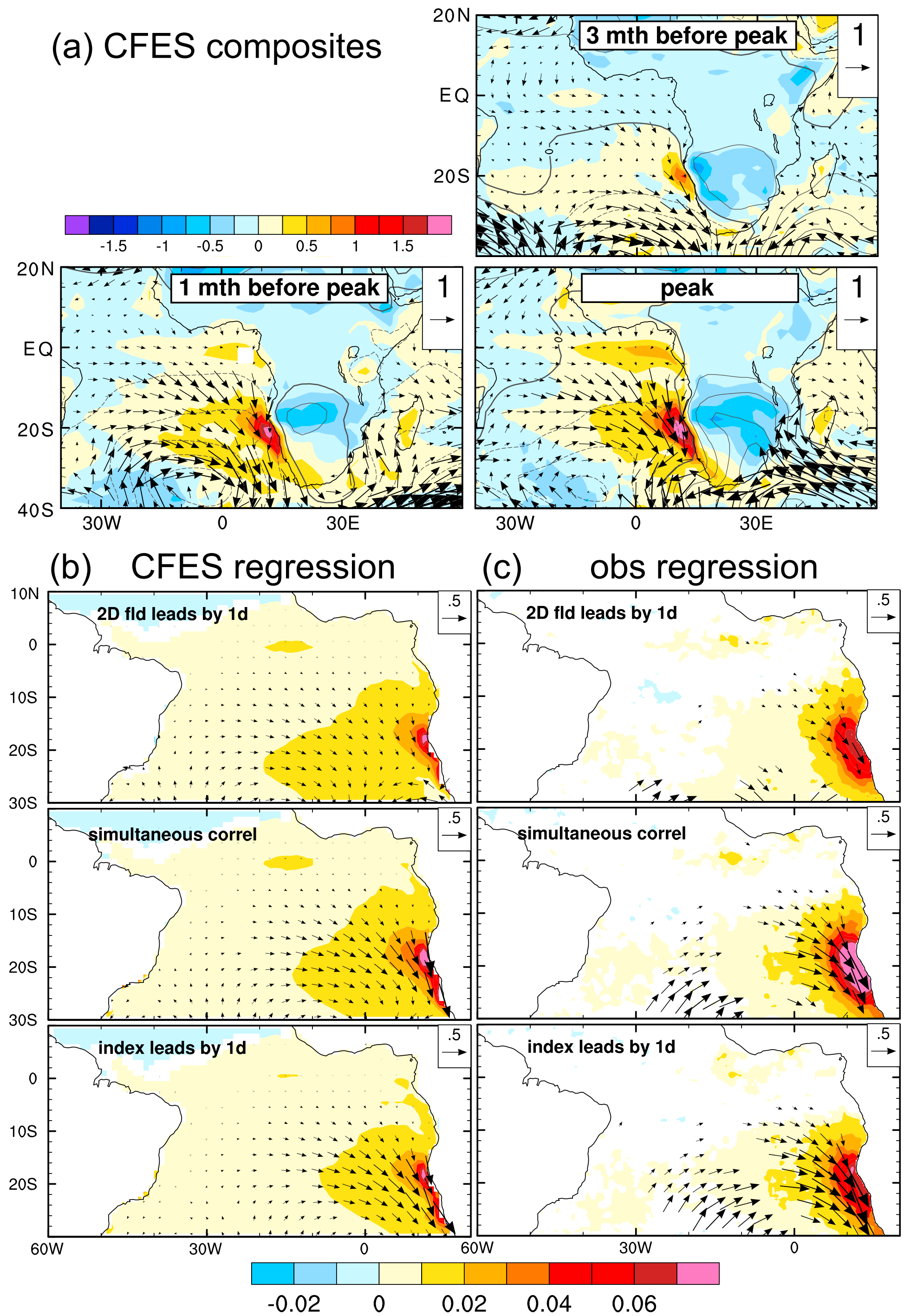

Figure 2. (a) Horizontal maps of simulated anomalous SST (shading; K; land areas indicate ground temperature), surface wind stress (arrows; N m^{-2}*100), and SLP (contours; 0.25 hPa interval) composited on the ABA SST index. Only events with standard deviations greater than 2 are selected. Dashed contour lines indicate negative values. (b and c) Regression coefficients obtained by regressing the normalized ABA index of daily mean SST tendency on SST tendency itself (shading; K/day) and surface winds (vectors; m/s). The left column shows CFES, the right column satellite observations. Regression is shown for time lags from −1 to +1 days, as indicated in the upper left.

[13] The simulated ABA SST anomalies are significantly correlated (at the 1% level) with indices of equatorial and along-shore wind stress anomalies. We define the equatorial index (EQA) as the zonal wind stress anomaly averaged over (40°W–10°W, 2°S–2°N) and the coastal index (AB2) as the meridional wind stress anomaly averaged over (8°E – coast, 30°S – equator). Using unfiltered weekly mean data, we find a correlation of −0.39 between ABA SST and AB2 wind stress when the latter leads by 1 week. When ABA instead of AB2 wind stress is used, the correlation reduces to −0.285 (1 week lag), indicating that anomalies equatorward of 15°S play a greater role than those directly over the

ABA. For the equatorial wind stress, the correlation is +0.311 but in this case the SSTs lead by 2 weeks. This might suggest that the EQA anomalies are a result of the equatorial Atlantic warming that typically follows Benguela Niños.

[14] For the satellite observations, the correlation between ABA SST and AB2 meridional wind stress is only −0.24 (when wind stress leads by one 1 week), which is significant at the 10% level. Other correlations are lower and not significant even at the 10% level. The reduced significance is likely due to the fact that the observation period is brief (9 years for QuikSCAT) and does not feature any pronounced events.

[15] We further examine the satellite observations and CFES simulation by regressing daily ABA SST tendency onto surface winds and SST tendency itself and plot the regression coefficients in Figures 2b and 2c. The results reveal that SST tendency along the southwestern African coast is highly sensitive to local wind stress anomalies on synoptic time scales in both CFES and observations. Figures 2b and 2c also illustrate that the surface wind anomalies implicated in the ABA SST changes are well aligned with the local coastline and thus very effective in reducing coastal upwelling. The large-scale pattern of wind stress anomalies, which extends far off-shore, is again suggestive of a weakened subtropical anticyclone as in Figure 2a, while the accompanying positive SST trends might be due to latent heat flux reduction. The results of the regression analysis are further supported by latitude time sections of daily mean SST and meridional wind stress anomalies (Figure S5 in Text S1 of the auxiliary material).

[16] We conclude our analysis with an examination of the 1995 Benguela Niño, which is the strongest event during the satellite observation period. Figure 1c (1d) shows daily longitude-time (latitude-time) sections of AVHRR SST and AVISO SSH anomalies (SSHA), where the latter are interpolated from weekly means. Positive SST anomalies around 16°S develop as early as October 1994 when SSH anomalies are still negative. In early February there is a sharp increase in SST that occurs almost simultaneously from 30°S to the equator. This is accompanied by positive SSHA at some latitudes but there is no indication of Kelvin wave propagation. Rather SSHA are organized in horizontal bands around 18°S, 12°S, and 7°S and thus appear to be stationary. Another, less pronounced, event in 2004 (not shown) features better evidence for Kelvin wave propagation but even there SSTA precede the advent of SSH anomalies.

4. Conclusions

[17] In the present study we have evaluated the relative importance of equatorial and along-shore wind anomalies in the development of Benguela Niños. Evidence based on both CGCM simulation results and observations indicates a crucial role for along-shore wind anomalies. These wind anomalies are part of a basin-scale weakening of the South Atlantic high that commences several months before SST anomalies peak. The large spatial coherence of this pattern can explain the observed high correlation between Benguela and Atlantic Niños (which is reproduced in the CGCM). The strong influence of along-shore winds is also apparent in a regression analysis of daily means for both model output and observations. SSTs respond to individual wind anomalies within a few days, and are particularly sensitive around 20°S. At first, it might seem that these synoptic time-scale fluctuations are not relevant to Benguela Niños (or their Benguela Niña counterparts), which develop over several months. The frequency and intensity of these wind anomalies, however, are subject to low-frequency modulation associated with changes in the strength of the subtropical high. It is this low-frequency modulation, which plays a crucial part in the development of Benguela Niños. This is analogous to Pacific Niños, which preferentially develop when westerly wind anomalies become more frequent and intense. Local air-sea interaction might further enhance the impact of individual along-shore wind bursts.

[18] Satellite observations of SST and SSH for the 1995 Benguela Niño show no evidence of a significant Kelvin wave influence. SSHA along the southwest African coast appear to be stationary rather than propagating poleward. Furthermore, SSHA are negative during the onset phase and do not become positive until the event matures.

[19] Our results concerning the weakening of the anticyclone are, in some sense, consistent with a study by *Trzaska et al.* [2007]. Using an AGCM coupled to a slab-ocean model, they found a quasi-biennial oscillation that involved weakening of the anticyclone and successive warming in the ABA and equatorial region. Their results, as well as ours, suggest that interannual variability in the South and Equatorial Atlantic can be excited by basin-scale changes in the subtropical high. Oceanic processes are, of course, necessary to achieve amplification of the signal in the upwelling regions.

[20] The role of the anticyclone has also been discussed in a recent study by *Lubbecke et al.* [2010]. Their study, however, emphasizes the equatorial influence of the anticyclone and invokes the Kelvin wave mechanism to explain the high correlation between Atlantic and Benguela Niños. The present study, in contrast, highlights the importance of local winds in the development of Benguela Niños and explains the correlation to Atlantic Niños with the large-scale weakening of the anticyclone that affects both areas simultaneously. While our results do not rule out an important role for Kelvin waves in the evolution of Atlantic warm events, the large spatial coherence of the wind stress forcing and the comparative smallness of the basin render their detection a challenge. This might not bode well for the potential utility of Kelvin wave signals in the prediction of Benguela Niños. However, the weakening of the subtropical high that precedes Atlantic warm events might offer hope for seasonal predictions as it develops 2–3 months ahead of Benguela Niños and 5–6 months ahead of Atlantic Niños. This underscores the importance of monitoring wind anomalies in the South Atlantic and particular along the southwest African coast. Continued monitoring in the latter region, would also allow to further clarify the influence of along-shore winds. Regarding the causes for the weakened subtropical high, some studies have indicated that conditions on the adjacent continents exert an important influence on the strength of the subtropical high [e.g., *Seager et al.*, 2003; *Richter et al.*, 2008]. Additionally, the position of the Atlantic ITCZ as well as remote influences from the Pacific and Indian Oceans are likely to contribute to the low-frequency modulation of the subtropical high. Further investigation is needed to evaluate the relative importance of these factors. The sensitivity of the coastal region to local

wind anomalies also opens up the possibility of a novel mode of air-sea interaction, which could not exist if Benguela Niños were purely remotely forced. This is the topic of current research efforts.

[21] **Acknowledgments.** The authors wish to thank Shang-Ping Xie, Tomoki Tozuka, Jing-Jia Luo, and Wataru Ohfuchi for helpful discussions. Thanks also to two anonymous reviewers for their constructive comments.

References

Bourlès, B., et al. (2008), The PIRATA program: History, accomplishments, and future directions, *Bull. Am. Meteorol. Soc.*, *89*, 1111–1125, doi:10.1175/2008BAMS2462.1.

Carton, J. A., G. Chepurin, X. Cao, and B. S. Giese (2000), A simple ocean data assimilation analysis of the global upper ocean 1950–1995, Part1: Methodology, *J. Phys. Oceanogr.*, *30*, 294–309, doi:10.1175/1520-0485(2000)030<0294:ASODAA>2.0.CO;2.

Davey, M. K., et al. (2002), STOIC: A study of coupled model climatology and variability in topical ocean regions, *Clim. Dyn.*, *18*, 403–420, doi:10.1007/s00382-001-0188-6.

Enomoto, T., A. Kuwano-Yoshida, N. Komori, and W. Ohfuchi (2008), Description of AFES 2: Improvements for high-resolution and coupled simulations, in *High Resolution Numerical Modelling of the Atmosphere and Ocean*, edited by K. Hamilton and W. Ohfuchi, pp. 77–97, Springer, New York.

Florenchie, P., J. R. E. Lutjeharms, C. J. C. Reason, S. Masson, and M. Rouault (2003), The source of Bengula Niños in the South Atlantic Ocean, *Geophys. Res. Lett.*, *30*(10), 1505, doi:10.1029/2003GL017172.

Florenchie, P., C. J. C. Reason, J. R. E. Lutjeharms, M. Rouault, C. Roy, and S. Masson (2004), Evolution of interannual warm and cold events in the southeast Atlantic Ocean, *J. Clim.*, *17*, 2318–2334, doi:10.1175/1520-0442(2004)017<2318:EOIWAC>2.0.CO;2.

Gnanadesikan, A., et al. (2006), GFDL's CM2 global coupled climate models. Part II: The baseline ocean simulation, *J. Clim.*, *19*, 675–697, doi:10.1175/JCLI3630.1.

Grodsky, S. A., J. A. Carton, and F. M. Bingham (2006), Low frequency variation of sea surface salinity in the tropical Atlantic, *Geophys. Res. Lett.*, *33*, L14604, doi:10.1029/2006GL026426.

Huang, B., and Z.-Z. Hu (2007), Cloud-SST feedback in southeastern tropical Atlantic anomalous events, *J. Geophys. Res.*, *112*, C03015, doi:10.1029/2006JC003626.

Komori, N., K. Takahashi, K. Komine, T. Motoi, X. Zhang, and G. Sagawa (2005), Description of sea-ice component of coupled Ocean–Sea-Ice Model for the Earth Simulator (OIFES), *J. Earth Simulator*, *4*, 31–45.

Komori, N., A. Kuwano-Yoshida, T. Enomoto, H. Sasaki, and W. Ohfuchi (2008), High-resolution simulation of the global coupled atmospheric-ocean system: Description and preliminary outcomes of CFES (CGCM for the Earth Simulator), in *High Resolution Numerical Modelling of the Atmosphere and Ocean*, edited by K. Hamilton and W. Ohfuchi, pp. 241–260, Springer, New York.

Kuwano-Yoshida, A., T. Enomoto, and W. Ohfuchi (2010), An improved PDF cloud scheme for climate simulations, *Q. J. R. Meteorol. Soc.*, *136*, 1583–1597, doi:10.1002/qj.660.

Lubbecke, J. F., C. W. Boning, N. S. Keenlyside, and S.-P. Xie (2010), On the connection between Benguela and equatorial Niños and the role of the South Atlantic Anticyclone, *J. Geophys. Res.*, *115*, C09015, doi:10.1029/2009JC005964.

Moore, D., P. Hisard, J. McCreary, J. Merle, J. O'Brien, J. Picaut, J.-M. Verstraete, and C. Wunsch (1978), Equatorial adjustment in the eastern Atlantic, *Geophys. Res. Lett.*, *5*, 637–640, doi:10.1029/GL005i008p00637.

Nonaka, M., H. Nakamura, B. Taguchi, N. Komori, A. Kuwano-Yoshida, and K. Takaya (2009), Air–sea heat exchanges characteristic of a prominent midlatitude oceanic front in the South Indian Ocean as simulated in a high-resolution coupled GCM, *J. Clim.*, *22*, 6515–6535, doi:10.1175/2009JCLI2960.1.

Numaguti, A., M. Takahashi, T. Nakajima, and A. Sumi (1997), Description of CCSR/NIES atmospheric general circulation model: Study on the climate system and mass transport by a climate model, in *CGER's Supercomput. Monogr. Rep. 3*, edited by A. Numaguti et al., pp. 1–48, Cent. for Global Environ. Res., Natl. Inst. for Environ. Stud., Tsukuba, Japan.

Ohfuchi, W., et al. (2004), 10-km mesh mesoscale resolving simulations of the global atmosphere on the Earth Simulator: Preliminary outcomes of AFES (AGCM for the Earth Simulator), *J. Earth Simulator*, *1*, 8–34.

Polo, I., A. Lazar, B. Rodriguez-Fonseca, and S. Arnault (2008a), Oceanic Kelvin waves and tropical Atlantic intraseasonal variability: 1. Kelvin wave characterization, *J. Geophys. Res.*, *113*, C07009, doi:10.1029/2007JC004495.

Polo, I., B. Rodríguez-Fonseca, T. Losada, and J. García-Serrano (2008b), Tropical Atlantic variability modes (1979–2002). Part I: time-evolving SST modes related to West African rainfall, *J. Clim.*, *21*, 6457–6475, doi:10.1175/2008JCLI2607.1.

Reason, C. J. C., and M. Rouault (2006), Sea surface temperature variability in the tropical southeast Atlantic Ocean and West African rainfall, *Geophys. Res. Lett.*, *33*, L21705, doi:10.1029/2006GL027145.

Richter, I., and S.-P. Xie (2008), On the origin of equatorial Atlantic biases in coupled general circulation models, *Clim. Dyn.*, *31*, 587–598, doi:10.1007/s00382-008-0364-z.

Richter, I., C. R. Mechoso, and A. W. Robertson (2008), What determines the position and intensity of the South Atlantic anticyclone in austral Winter?—An AGCM study, *J. Clim.*, *21*, 214–229, doi:10.1175/2007JCLI1802.1.

Rouault, M., S. Illig, C. Bartholomae, C. J. C. Reason, and A. Bentamy (2007), Propagation and origin of warm anomalies in the Angola Benguela upwelling system in 2001, *J. Mar. Syst.*, *68*, 473–488, doi:10.1016/j.jmarsys.2006.11.010.

Seager, R., R. Murtugudde, N. Naik, A. Clement, N. Gordon, and J. Miller (2003), Air–sea interaction and the seasonal cycle of the subtropical anticyclones, *J. Clim.*, *16*, 1948–1966, doi:10.1175/1520-0442(2003)016<1948:AIATSC>2.0.CO;2.

Servain, J., A. J. Busalacchi, M. J. McPhaden, A. D. Moura, G. Reverdin, M. Vianna, and S. E. Zebiak (1998), A Pilot Research Moored Array in the Tropical Atlantic (PIRATA), *Bull. Am. Meteorol. Soc.*, *79*, 2019–2031, doi:10.1175/1520-0477(1998)079<2019:APRMAI>2.0.CO;2.

Shannon, L. V., A. J. Boyd, G. B. Bundrit, and J. Taunton-Clark (1986), On the existence of an El Niño–type phenomenon in the Benguela system, *J. Mar. Sci.*, *44*, 495–520.

Trzaska, S., A. W. Robertson, J. D. Farrara, and C. R. Mechoso (2007), South Atlantic variability arising from air–sea coupling: Local mechanisms and tropical–subtropical interactions, *J. Clim.*, *20*, 3345–3365, doi:10.1175/JCLI4114.1.

Yamagata, T., and S. Iizuka (1995), Simulation of the tropical thermal domes in the Atlantic: A seasonal cycle, *J. Phys. Oceanogr.*, *25*, 2129–2140, doi:10.1175/1520-0485(1995)025<2129:SOTTTD>2.0.CO;2.

S. K. Behera, Y. Masumoto, and I. Richter, Research Institute for Global Change, JAMSTEC, 3173-25 Showa-machi, Kanazawa-ku, Yokohama, Kanagawa 236-0001, Japan. (richter@jamstec.go.jp)

N. Komori and B. Taguchi, Earth Simulator Center, JAMSTEC, 3173-25 Showa-machi, Kanazawa-ku, Yokohama, Kanagawa 236-0001, Japan.

T. Yamagata, Application Laboratory, JAMSTEC, 3173-25 Showa-machi, Kanazawa-ku, Yokohama, Kanagawa 236-0001, Japan.